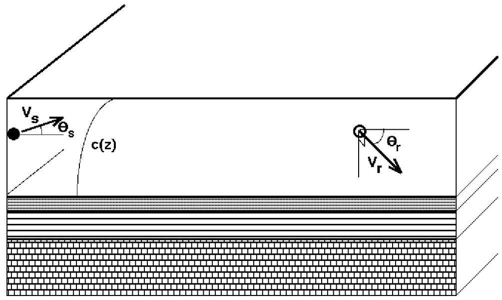

Fig. 8.2. Horizontally stratified ocean with horizontally moving source and receiver. The source is moving at speed v_s and bearing θ_s, while the receiver is moving at speed v_r and bearing θ_r. Vertical motion is ignored.

8.4 Doppler Shift in a Waveguide

Up to this point, we have discussed only solutions to the wave equation for stationary problems, i.e., for the environment and source/receiver configuration fixed throughout the duration of the propagation. However, for real sonar environments, this is not always a valid assumption. Thus, we shall demonstrate in the following that the problem of a moving source or receiver is of broadband nature, even for a monochromatic CW source.

It is well known that a moving source and/or receiver in free space results in a frequency Doppler shift which is described by the simple relation obtained from a Galilean transformation [11]. In a waveguide or stratified environment, source/receiver motion results in a more complicated Doppler structure because of multipath phenomena. Here we consider the simplest case: horizontal motion in a range-independent waveguide environment; each horizontal wavenumber component of the acoustic field will undergo a different Doppler shift. Previous waveguide derivations [19, 20] used normal-mode representations for deriving the Doppler shifted field. Here we present a simple derivation based on the spectral representation in a form which requires only a very simple modification of an existing wavenumber integration code to incorporate the source/receiver dynamics. The spectral formulation is then translated into a numerically tractable modal formulation.

We start with the wave equation governing the field produced by a moving source in a horizontally stratified ocean, as shown in Fig. 8.2. As we shall see later, once the expression for the field is found for the moving source, it is straightforwardly modified to incorporate receiver motion. The wave equation (2.25) in cartesian coordinates, with the right-hand-side representing a harmonic point source of time dependence

$\exp(-i\Omega t)$ and moving with a constant horizontal velocity vector $\mathbf{v}_s$, is

$$\nabla^2\psi(\mathbf{r},z,t) - \frac{1}{c^2}\frac{\partial^2\psi(\mathbf{r},z,t)}{\partial t^2} = -\delta(\mathbf{r}-\mathbf{v}_s t)\,\delta(z-z_s)\,e^{-i\Omega t}\,. \tag{8.43}$$

We now apply the Fourier transform in Eq. (2.27) to arrive at the inhomogeneous Helmholtz equation,

$$\left[\nabla^2 + k_\omega^2\right]\psi(\mathbf{r},z,\omega) = -\delta(z-z_s)\int\delta(\mathbf{r}-\mathbf{v}_s t)\,e^{i(\omega-\Omega)t}dt\,, \tag{8.44}$$

where k_ω is the medium wavenumber at frequency ω, $k_\omega = \omega/c$. In the following we will first derive the wavenumber integral representation for the solutions to Eq. (8.44), followed by the normal mode equivalent.

8.4.1 Wavenumber Integral Representation

Because of the source motion, we do not assume the problem to be axisymmetric; rather than the Hankel transforms used in Sec. 2.4, we use a two-dimensional Fourier transform to reduce the spatial dimension of the Helmholtz equation. Thus, we use the transform pair

$$\psi(\mathbf{r},z;\omega) = \int\psi(\mathbf{k_r},z;\omega)\,e^{i\mathbf{k_r}\cdot\mathbf{r}}\,d^2\mathbf{k_r}\,, \tag{8.45}$$

$$\psi(\mathbf{k_r},z;\omega) = \frac{1}{(2\pi)^2}\int\psi(\mathbf{r},z;\omega)\,e^{-i\mathbf{k_r}\cdot\mathbf{r}}\,d^2\mathbf{r}\,, \tag{8.46}$$

to transform Eq. (8.44) into the depth-separated wave equation,

$$\begin{aligned}\frac{d^2\psi(\mathbf{k_r},z;\omega)}{dz} + \left[k_\omega^2 - k_r^2\right]\psi(\mathbf{k_r},z;\omega) &= -\frac{\delta(z-z_s)}{(2\pi)^2}\int e^{i(\omega-\Omega-\mathbf{k_r}\cdot\mathbf{v}_s)t}\,dt \\ &= -\frac{\delta(z-z_s)}{2\pi}\,\delta(\omega-\Omega-\mathbf{k_r}\cdot\mathbf{v}_s)\,,\end{aligned} \tag{8.47}$$

with $k_r = |\mathbf{k_r}|$, and where we have used the identities

$$\int\delta(\mathbf{r}-\mathbf{v}_s t)\,e^{-i\mathbf{k_r}\cdot\mathbf{r}}\,d^2\mathbf{r} = e^{-\mathbf{k_r}\cdot\mathbf{v}_s t}\,, \tag{8.48}$$

and

$$\frac{1}{2\pi}\int e^{i(\omega-\Omega-\mathbf{k_r}\cdot\mathbf{v}_s)\,t}\,dt = \delta(\omega-\Omega-\mathbf{k_r}\cdot\mathbf{v}_s)\,. \tag{8.49}$$

Equation (8.47) is a standard depth-separated wave equation of the form given in Eq. (4.3), with the solution

$$\psi(\mathbf{k_r}, z; \omega) = \delta(\omega - \Omega - \mathbf{k_r} \cdot \mathbf{v}_s)\, g(k_r, z; \omega)\,, \tag{8.50}$$

with $g(k_r, z; \omega)$ being the depth-dependent Green's function for the waveguide at frequency ω, satisfying Eq. (2.90), and being determined for arbitrary stratifications by any of the methods described in Chap. 4.

The time-domain solution then follows by evaluation of the inverse Fourier transforms in Eqs. (8.45) and (2.26),

$$\psi(\mathbf{r}, z, t) = \frac{1}{2\pi} \int e^{-i\omega t}\, d\omega \int \psi(\mathbf{k_r}, z, \omega)\, e^{i\mathbf{k_r}\cdot\mathbf{r}}\, d^2\mathbf{k_r}\,, \tag{8.51}$$

which by insertion of Eq. (8.50) reduces to

$$\psi(\mathbf{r}, z, t) = \frac{1}{2\pi} \int g(k_r, z; \Omega + \mathbf{k_r} \cdot \mathbf{v}_s)\, e^{-i[(\Omega + \mathbf{k_r}\cdot\mathbf{v}_s)t - \mathbf{k_r}\cdot\mathbf{r}]}\, d^2\mathbf{k_r}\,. \tag{8.52}$$

Thus, in evaluating the integral, we simply have to compute the depth-dependent Green's function for each wave vector $\mathbf{k_r}$ at the frequency

$$\omega = \Omega + \mathbf{k_r} \cdot \mathbf{v}_s\,. \tag{8.53}$$

Equation (8.53) represents the *Doppler frequency shift* for each wavenumber component of the field resulting from a moving harmonic source. Now, it is clear that since the expression in Eq. (8.52) represents the field at all range vectors $\mathbf{r}$, we can straightforwardly modify it to include the receiver motion. Thus, the range vector for a receiver at position $\mathbf{r}_0$ at time $t = 0$, and moving with a velocity vector $\mathbf{v}_r$, is given by $\mathbf{r} = \mathbf{r}_0 + \mathbf{v}_r t$. Insertion of this into Eq. (8.52) yields

$$\psi(\mathbf{r}_0 + \mathbf{v}_r t, z, t) = \frac{1}{2\pi} \int g(k_r, z; \Omega + \mathbf{k_r} \cdot \mathbf{v}_s)\, e^{-i\left[[\Omega + \mathbf{k_r}\cdot(\mathbf{v}_s - \mathbf{v}_r)]t - \mathbf{k_r}\cdot\mathbf{r}_0\right]}\, d^2\mathbf{k_r}\,. \tag{8.54}$$

Here, it is interesting to note the asymmetry between source and receiver motion. Thus, whereas both source and receiver motion yield a frequency shift through the exponential, only the source motion affects the integration kernel, i.e., the depth-dependent Green's function. Therefore, reciprocity does not hold for moving sources and receivers! Also note that, as expected, no Doppler shift is observed if source and receiver are moving at identical velocities, but the kernel is still affected, in a non-reciprocal way.

Therefore, the field observed at a receiver moving with the same speed and direction as the source is different from the field observed in the stationary case, a fact which is rarely appreciated when interpreting experimental data. On the other hand, as we shal demonstrate this effect is rather small, making the static approximation valid for most realistic source/receiver motions. A joint source/receiver motion is clearly equivalent to stationary sources and receivers in a moving medium.

Even though Eq. (8.54) represents the field through a wavenumber integral, this expression is not well suited for direct numerical implementation. The reason is that the source/receiver dynamics couples the time and wavenumber through the argument to the exponential function, requiring the integral to be evaluated for each individual time value. However, it turns out that this time-wavenumber coupling is closely tied to the formulation in the *source's* frame of reference, i.e. in terms of a harmonic source excitation of frequency Ω, resulting in each received wavenumber component to be of different frequency. Thus, as shown by Schmidt and Kuperman [21] a much simpler, and numerically tractable, formulation is achieved by assuming the source to have a finite bandwidth, which is obviously realistic, and transforming the field expression in Eq. 8.54 into the *receiver's* frame of reference. For a source with finite bandwidth $S(\Omega)$, the field at the receiver is simply determined by a Fourier integral of the above expressions,

$$\begin{aligned}\psi(\mathbf{r}_0 + \mathbf{v}_r t, z, t) = & \frac{1}{4\pi^2} \int d\Omega S(\Omega) \int d^2\mathbf{k_r} \\ & \times G(k_r, z; \Omega + \mathbf{k_r} \cdot \mathbf{v}_s) e^{-i[(\Omega + \mathbf{k_r}\cdot(\mathbf{v}_s - \mathbf{v}_r))t - \mathbf{k_r}\cdot\mathbf{r}_0]} \,. \end{aligned} \tag{8.55}$$

In the receiver's frame of reference the frequency spectrum of the field at the receiver now follows by applying the Fourier transform in Eq. (2.27) to Eq. (8.55),

$$\begin{aligned}\psi(\mathbf{r}_0 + \mathbf{v}_r t, z, \omega) &= \int dt e^{i\omega t} \psi(\mathbf{r}_0 + \mathbf{v}_r t, z, t) \\ &= \frac{1}{4\pi^2} \int d\Omega S(\Omega) \int d^2\mathbf{k_r} e^{i\mathbf{k_r}\cdot\mathbf{r}_0} G(k_r, z; \Omega + \mathbf{k_r}\cdot\mathbf{v}_s) \\ &\quad \times \int dt e^{-i(\Omega - \omega + \mathbf{k_r}\cdot(\mathbf{v}_s - \mathbf{v}_r))t} \\ &= \frac{1}{2\pi} \int d^2\mathbf{k_r} e^{i\mathbf{k_r}\cdot\mathbf{r}_0} \int d\Omega S(\Omega) \\ &\quad \times G(k_r, z; \Omega + \mathbf{k_r}\cdot\mathbf{v}_s) \delta(\Omega - \omega + \mathbf{k_r}\cdot(\mathbf{v}_s - \mathbf{v}_r)) \\ &= \frac{1}{2\pi} \int d^2\mathbf{k_r} e^{i\mathbf{k_r}\cdot\mathbf{r}_0} S(\Omega_k) G(k_r, z; \omega + \mathbf{k_r}\cdot\mathbf{v}_r) \,, \end{aligned} \tag{8.56}$$

where Ω_k is the Doppler shifted source frequency

$$\Omega_k = \omega - \mathbf{k_r} \cdot (\mathbf{v}_s - \mathbf{v}_r) \,. \tag{8.57}$$

Equation (8.56) represents stationary frequency components of the field in the receiver's frame of reference, with the time domain response following by evaluation of the inverse Fourier transform in Eq. (2.26). Thus, simply by transforming into the receiver's frame of reference, i.e. changing from a representation in terms of "source frequency" Ω in Eq. (8.55) to a representation in terms of "receiver frequency" ω, the coupling between time and wavenumber has been eliminated. As a result, the wavenumber and frequency integrations are performed independently, as in the static case. In fact, the differences introduced by the dynamics are rather trivial. The first concerns the source spectrum $S(\Omega_k)$ which is wavenumber-independent in the static case and therefore in that case may be applied outside the wavenumber integral, as part of the Fourier synthesis; the other difference is the change in frequency-argument to the depth-dependent Green's function. We will later discuss the physical significance of these differences.

In spite of its extraordinary simplicity, Eq. (8.56) is *exact* within the limitations of the linear theory of acoustics. Thus, the only assumption made is that source and receiver are moving at constant speed.

Unfortunately, the evaluation of the two-dimensional wavenumber integral in Eq. (8.56) is computationally intensive. However, in underwater acoustics the range separation of the source and receiver is usually large compared to the track of each during the time duration of the signal. The angles θ_s and θ_r between the velocity vectors of the source and receiver, respectively, and the radial vector connecting them, can therefore be considered constant, and we can replace the 2-D Fourier integral in Eq. (8.56) by a Hankel transform representation in the horizontal wavenumber [22], i.e.

$$\begin{aligned} &\psi(\mathbf{r}_0 + \mathbf{v}_r t, z, \omega) \\ &\quad \simeq \int_0^\infty dk_r k_r J_0(k_r r_0) \\ &\qquad\quad \times S(\Omega_k) G(k_r, z; \omega + k_r v_r \cos\theta_r) \\ &\quad = \frac{1}{2}\int_{-\infty}^\infty dk_r k_r H_0^{(1)}(k_r r_0) \\ &\qquad\quad \times S(\Omega_k) G(k_r, z; \omega + k_r v_r \cos\theta_r)\,, \end{aligned} \tag{8.58}$$

with

$$\Omega_k = \omega - k_r(v_s\cos\theta_s - v_r\cos\theta_r)\,. \tag{8.59}$$

Using this approximation it is extremely simple to modify an existing wavenumber integration code to compute the Doppler shifted acoustic field. The only change needed is to compute the depth-dependent Green's function at the shifted frequency $\omega + k_r v_r \cos\theta_r$ for every wavenumber k_r considered, and multiply it by the source spectrum at the shifted frequency Ω_k. The resulting dynamic transfer functions are then transformed into the time domain response by standard Fourier synthesis.

8.4.2 Normal Mode Representation

Based on the spectral representations given above it is now straightforward to proceed to the normal mode representation of the doppler shifted discrete part of the acoustic field. Ignoring the branch line contribution, the depth-dependent Green's function can be written in terms of normal modes through Eq. (5.40),

$$G(k_r, z; \omega) \simeq \frac{1}{2\pi\rho(z_s)} \sum \frac{\Psi_n(z)\Psi_n(z_s)}{k_r^2 - k_n^2}, \tag{8.60}$$

where k_n are the eigenvalues of the homogeneous form of Eq. (8.47), and Ψ_n are the associated eigenvectors. We can now replace the kernel in Eq. (8.58) by the modal expansion in Eq. (8.60), but with the wavenumber k_n replaced by the eigenvalues k_n^* at doppler shifted frequency $\omega + k_n v_r \cos\theta_r$, i.e. for $v_r/c \ll 1$,

$$k_n^* \simeq k_n \left(1 + v_r \cos\theta_r \frac{dk_n}{d\omega}\right) = k_n \left(1 + \frac{v_r}{v_{ng}} \cos\theta_r\right), \tag{8.61}$$

where v_{ng} is the *group velocity* of the $n-th$ mode at angular frequency ω. The wavenumber integral in Eq. (8.58) can then, in analogy to the static case, be replaced by the modal sum,

$$\begin{aligned} \psi(\mathbf{r}_0 + \mathbf{v}_r t, z, \omega) &\simeq \frac{i}{4\rho(z_s)} \sum_n S(\Omega_n) \\ &\times \Psi_n(z)\Psi_n(z_s) H_0^{(1)}\left(k_n r_0 (1 + \tfrac{v_r}{v_{ng}} \cos\theta_r)\right), \end{aligned} \tag{8.62}$$

where

$$\begin{aligned} \Omega_n &= \omega - k_n(v_s \cos\theta_s - v_r \cos\theta_r) \\ &= \omega \left(1 - \frac{v_s}{v_{np}} \cos\theta_s + \frac{v_r}{v_{np}} \cos\theta_r\right), \end{aligned} \tag{8.63}$$

with $v_{np} = \omega/k_n$ being the modal *phase velocity*. Here it has been assumed that the change in modal eigenfunctions is negligable. Further, this expression ignores any modal cutoff effects introduced by the doppler shift, and as such Eq. (8.62) represents another level of approximation compared to the spectral representation in Eq. (8.58). On the other hand, the physical interpretation of the dynamic effects is very simple in the modal approximation. It is clear from Eq. (8.63) that the doppler shift in observed frequency is associated with the horizontal *phase velocity* of the individual modes. Since each mode is a result of the constructive interference of up- and down-going plane waves with distinct grazing angles $\phi_n = \cos^{-1}(k_n/k_w)$, different modes clearly have different phase velocities and therefore different doppler shifts.

The source/receiver dynamics also yields a perturbation in the interference associated with the change in the modal propagation wavenumbers in Eq. (8.61). It is clear from Eq. (8.62) that this change in modal eigenvalue can alternatively be interpreted as a change in range. With this observation we can easily interprete this effect physically as being associated with the different distances the modes are traveling from being launched at the source to being received at the receiver, due to their different *group velocities*. Here it is interesting to note that this effect only involves the receiver motion. However, this asymmetry, which is the reason for the earlier discussed lack of reciprocity, actually makes sense physically. Assume the source function is a delta function in time, i.e. $S(\Omega) \equiv 1$. All modes in the waveguide will then be excited at the same instance in time, and their arrival time and therefore relative phase will be unaffected by the continued source motion. Therefore, if the receiver is at rest, the arrival time, and therefore relative phase, of the modes is independent of the source dynamics. On the other hand, if the receiver is moving, it will pick up the individual modal arrivals at different points in space due to their different group velocities. As a result, the relative phase between the modes is affected, reflected through the change in observed modal wavenumber given in Eq. (8.61). This *wavenumber doppler shift* was ignored in the doppler formulation of Fawcett and Maranda [23], but as is clear from Eqs. (8.62) and (8.63), this effect can be equally important to the *frequency doppler shift*, depending on the ratio between the relative source/receiver speed and the receiver speed itself.

It is easily verified, that for a stationary receiver and a moving, monochromatic source, $S(\Omega) = \delta(\Omega - \Omega_0)$, the Fourier transform of Eq. (8.63) becomes identical to the expressions derived by Guthrie *et al.* [19] and Hawker [20] for this special case. Their results could also be derived by directly replacing the wavenumber integral in Eq. (8.52) by its modal expansion.

Next, we will derive a simple modification of the adiabatic mode expansion, incorporating the source/receiver dynamics. This is easily done heuristically, based on the physical interpretation of the two effects of the dynamics stated above. For the static case the adiabatic expansion of the field produced by a source of strength $S(\omega)$ directly follows from Eq. (5.191) as

$$\psi(r,z,\omega) \simeq \frac{iS(\omega)e^{-i\pi/4}}{\rho(z_s)\sqrt{8\pi}} \sum_n \Psi_n(z)\Psi_n(z_s) \frac{e^{i\int_0^r k_n(r')dr'}}{\sqrt{\int_0^r k_n(r')dr'}} \,. \tag{8.64}$$

Now it is clear from the above that the frequency doppler shift depends on the phase velocities at the source and receiver, whereas the phase shift is associated with the different ranges the modes are traveling before reaching the moving receiver. Based on this observation, the adiabatic result directly follows as

$$\psi(\mathbf{r}_0+\mathbf{v}_r t, z, \omega) \simeq$$
$$\frac{ie^{-i\pi/4}}{\rho(z_s)\sqrt{8\pi}} \sum_n S(\Omega_n^*)\Psi_n(z)\Psi_n(z_s)\frac{e^{i\int_0^{r_n^*} k_n(r')dr'}}{\sqrt{\int_0^{r_n^*} k_n(r')dr'}} \ . \tag{8.65}$$

where

$$\Omega_n^* = \omega\left(1-\frac{v_s}{v_{np}(0)}\cos\theta_s + \frac{v_r}{v_{np}(r_0)}\cos\theta_r\right) \ , \tag{8.66}$$

and r_n^* is the perturbed ranges for the phase integrals,

$$r_n^* = r_0\left(1+\frac{v_r}{v_{ng}(r_0)}\cos\theta_r\right) \ . \tag{8.67}$$

The modification of existing normal mode codes to account for the source/receiver dynamics is clearly equally simple to the one described above for wavenumber integration codes.

8.5 Numerical Examples

This section presents a few examples of the kind of detailed insight into ocean-acoustic propagation which can be achieved only through time-series analysis. The geophysics literature is replete with references showing that even extremely complicated arrival structures in heterogeneous fluid–elastic environments can be completely untangled by exploiting the different propagation characteristics of the various wave types. Thus, it is often possible to explicitly identify compressional (p) and shear bulk waves (sh, sv), various converted components of these waves, head waves, guided p and s modes, interface waves, $etc.$ For illustrative examples we refer the reader to two recent publications dealing with the modeling aspect of seismic wave propagation: Schmidt and Tango [8] describe a pulse modeling technique for horizontally stratified media based on the wavenumber integration technique (Chap. 4) combined with Fourier synthesis; Dougherty and Stephen [12] present time-domain finite-difference solutions for range-dependent elastic media.

We shall concentrate on some fundamental aspects of acoustic propagation in both shallow and deep water. The problems are solved both in the time domain and via Fourier synthesis, and results are presented either as stacked time series versus range or depth, or as snapshots at fixed times.